A novel jet-loop anaerobic filter membrane bioreactor treating raw slaughterhouse wastewater: biological and filtration processes.

V. Diez[a]*, J.M. Cámara[b], M.O. Ruiz[a], R. Martínez[a], C. Ramos[a]

[a] Department of Biotechnology and Food Science, Chemical Engineering Division. University of Burgos, Plaza Misael Bañuelos, 09001 Burgos, Spain.

[b] Department of Electromechanical Engineering, Electronics Technology Division. University of Burgos, Avda. Cantabria s/n, 09006 Burgos, Spain.

*Corresponding author. Tel.: +34 947497017 E−mail address: vdiezb@ubu.es

Abstract

Results from raw slaughterhouse wastewater treatment in a new jet-loop Anaerobic Filter Membrane Bioreactor (AnFMBR) are presented. The innovation consists in integrating an attached growth anaerobic reactor and a filtration tank as an external loop gas-lift bioreactor, taking advantage of the gas-lift effect caused by the gas sparging used for fouling mitigation. A jet-loop AnFMBR pilot plant was operated for 18 months with a hydraulic retention time of 19.5–21.3 h, a solid retention time of 60 d and organic loading rates between 3.5–7.4 kg COD/m^3·d, depending on the wastewater concentration, with peaks of up to 10.9 kg COD/m^3·d. Organic matter removal efficiency was maintained between 92 and 97%. Most of the biomass in the jet-loop AnFMBR, 82%, was retained by the carrier material so the membrane was in contact with low concentration biomass suspension.

Effects of different backwash scenarios and filtration fluxes on reversible and irreversible fouling rates were studied by short-term and mid-term assays, using Box-Behnken experimental designs. Fouling consolidation due to the fouling layer compression was the main cause of irreversible fouling. Pilot-scale results have shown that jet-loop AnFMBR is a promising technology for real scale complex wastewater treatment.

1   INTRODUCTION

Food industry wastewaters in general, including slaughterhouse wastewaters, usually have high levels of biodegradable organic matter and suspended solids [1]. Biogas generation, low sludge production and substantial foot print savings, make anaerobic digestion an attractive technology for the treatment of food industry wastewaters [2]. However, complex wastewaters containing 30–70% of organic matter as particulate organics might cause operational problems in conventional high-rate anaerobic bioreactors [3,4]. Accumulation of undegraded suspended solids in high-rate anaerobic bioreactors leads to the decrease of solids retention time and reactors' efficiency, due to the increase of non-viable solids, sludge lifting, scum formation and washout of lighter flocs [5]. Long chain fatty acids, generated from the rupture of fat molecules, can exert significant biological problems in the anaerobic processes [6]. Sludge flotation or unsuccessful granulation and therefore operational failure of UASB-type reactors has been reported in the treatment of industrial wastewater with high lipid contents [7–9]. Treatment of wastewater containing high levels of slowly biodegradable organic matter such as particulate organic matter, oil and grease and colloidal matter can be addressed

2

by a two-phase hydrolysis-UASB approach. In this manner, slowly biodegradable materials are pre-hydrolysed and acidified without losing methanogenic potential, then the resulting soluble organic matter can be treated in the UASB [4]. However, the presence of harmful components for the biological treatment is often prevented by means of physicochemical pre-treatments. From an economic point of view, physicochemical pre-treatments increase sludge management cost and reduce biogas production, but from a technical point of view, operational problems related to sludge flotation or defective granulation are avoided. Another way to avoid the problems associated with unfavourable characteristics of the wastewater is to use membranes not affected by the accumulation of slowly biodegradable particles, the sludge settleability or by biomass degranulation [10]. The combination of anaerobic treatment processes and membrane technology takes the advantages of both processes. Anaerobic processes are considered the most suitable biological technology for the treatment of high strength wastewaters, whereas, for the removal of low biodegradable matter from complex industrial wastewaters, membrane-based processes have been identified as the most suitable physico-chemical technology [11]. However, the combination of membrane and anaerobic processes is not a mature technology yet. Practical implementation details may lead to some difficulties. Most types of anaerobic reactors have been combined with membrane technologies, being the most commonly used the completely mixed anaerobic digesters and UASB-type reactors [12].

Anaerobic filter (AF) technology, is based on biomass retention on the inert support material of a fixed bed. In the AF reactors, particles and organic matter from the wastewater are trapped and degraded by the active biomass that remains attached on the carrier material surface, or suspended in the interstitial void spaces [13]. AF has been

successfully used to treat different high strength wastewaters such as beet sugar [14], slaughterhouse [15,16], meat and dairy industries [17,18], distillery waste [19] and vinasse [20]. An option to improve the effluent quality could be to combine AF technology with membrane bioreactors (MBR), creating a hybrid system [2,21], or an integrated anaerobic system [22]. Fixed-bed AnMBR might improve the removal efficiency and reduce filtration resistance through the retention of sludge in the carrier material [21,23]. The main obstacles of both technologies, long start–up periods and clogging issues of AF reactors [24], and membrane fouling of AnMBRs [25], can be removed when AF and AnMBR are combined. The membrane guarantees biomass retention, which in turn facilitates biofilm formation on the support media and shortens the start-up period. Clogging issues are effectively controlled by adjusting the superficial velocity. Meanwhile, membrane fouling is mitigated because the concentration of sludge in contact with the membrane is reduced due to biomass retention in the AF.

In a previous work, an anaerobic filter and an ultrafiltration membrane submerged in the riser section of an internal loop gas–lift bioreactor, was presented [22]. A quick start-up was carried out and an organic loading rate, OLR, of 7 kg COD/$m^3 \cdot$d was reached in just two weeks, using a filtration flux of 15.7–17.1 L/$m^2 \cdot$h. The integration of the filtration tank in an inner chamber inside the anaerobic filter simplifies construction but has an important operational drawback: the chemical cleaning of the membrane cannot be performed *in situ*.

Several issues have been reported on the anaerobic treatment of raw slaughterhouse wastewater, both in anaerobic filter reactors [15] and in anaerobic membrane bioreactors [26]. The high content of suspended and colloidal components might deteriorate the microbial activity, washout active biomass, or lead to clogging in AFs

reactors. On the other hand, suspended and colloidal matter can aggravate membrane fouling in AnMBRs.

The performance of a novel membrane bioreactor, named jet-loop anaerobic filter membrane bioreactor (AnFMBR), was studied in the treatment of raw slaughterhouse wastewater. The novel jet-loop AnFMBR integrates a down-flow anaerobic fixed bed reactor and an ultrafiltration stage by submerged membranes to produce a high-quality effluent and biogas from complex wastewaters. The recirculation between both stages takes advantage of the gas–lift effect caused by the gas sparging used for membrane fouling mitigation, without additional recirculation pumps. The aim of the present paper is to evaluate the concentration and methanogenic activity of the attached and suspended biomass of the anaerobic filter, and the influence of filtration flux, and frequency, duration and flux of backwashing on the reversible and irreversible membrane fouling rates. Response surface methodology was used to analyse the individual and combined effects of the studied variables using short-term and mid-term assays.

2   MATERIALS AND METHODS

2.1   Jet-loop anaerobic filter membrane bioreactor

The flow scheme of the jet-loop AnFMBR is illustrated in Figure 1. The jet-loop AnFMBR consisted of a 0.18 m^3 downflow anaerobic filter filled with plastic carriers (Biofill–C, Bio–fil) for biomass immobilization, and a 0.016 m^3 upflow filtration tank where a submerged hollow fibre PVDF membrane (Zenon Zeweed–10) was placed. The specific surface of support media was $460 \text{ m}^2/\text{m}^3$, with a porosity of 90%. The filtration area of the membrane was 0.93 m^2. The pore size, 0.04 μm, was about ten times smaller than the size of bacteria, and the hydrophilic surface tends to prevent the membrane fouling.

Biological and filtration tanks were connected to each other at the bottom and at upper parts to allow mixed liquor recirculation. The biogas produced by the biological process, collected from the upper part of the biological tank, was recirculated by a diaphragm compressor (Secoh SV50) for the membrane scouring. Gas sparging caused an upwards flow of the retentate by gas–lift effect, overflowing on the top of the biological tank without the need for using electromechanical pumping devices for the mixed liquor recirculation. The mixed liquor flowed downwards through the plastic carriers towards the bottom, and returned to the filtration tank, closing the jet-loop circuit. A butterfly valve in the lower pipe enabled to isolate the filtration tank for in-situ chemical cleaning of the membrane.
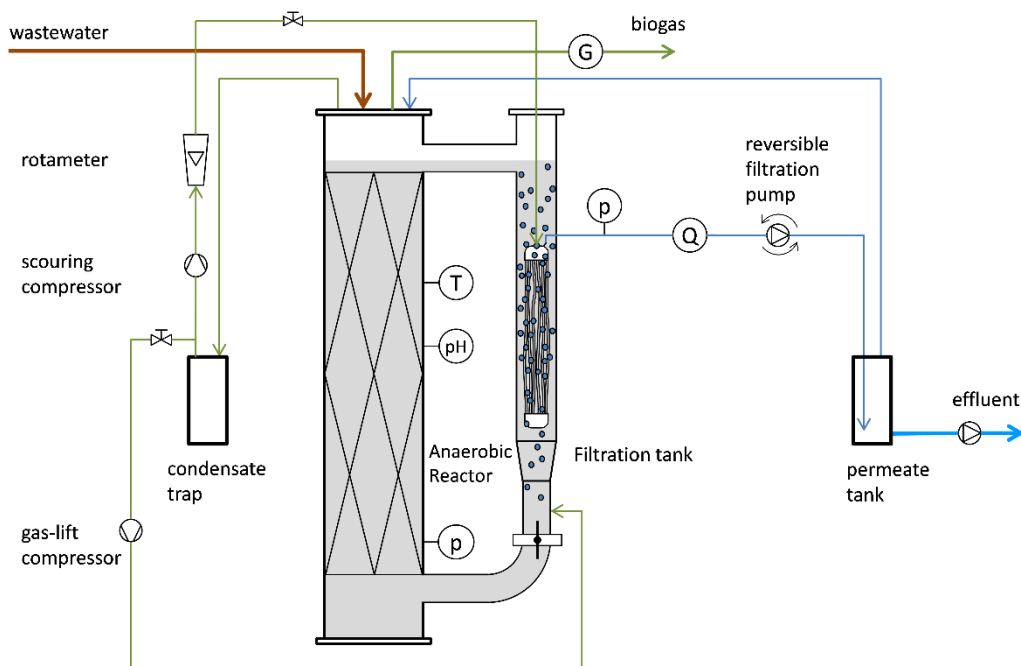

Figure 1. Schematic diagram of the jet-loop Anaerobic Filter Membrane Bioreactor. G: biogas flow meter, p: pressure sensor, pH: pH sensor, Q: permeate flow meter, T: temperature sensor.

A peristaltic pump (Watson Marlow 520U) introduced raw slaughterhouse wastewater through the upper part of the anaerobic filter. A reversible wear pump (Micropump Eagle

Drive GJ–N21) was used for filtration and backwashing. This pump was connected to a 1 L tank that collects membrane permeate for backwashing. Another peristaltic pump (Watson Marlow 520U) was employed for effluent withdrawal from the permeate vessel, while the permeate excess was returned to the head space of the anaerobic filter. The wastewater feed pump was controlled by the effluent withdrawal, so the control of the hydraulic retention time, HRT, and OLR of the biological process, were independent of the filtration flux. 3 L of sludge from the filtration tank was daily wasted to maintain a 60 d solids retention time, SRT, on suspended biomass basis.

Temperature of biological process was kept at 30±1.0 ºC by means of an electric blanket heating. Electronic pressure sensors (PN 2569, IFM) monitored transmembrane pressure (TMP) and reactor filling level. Filtration and backwashing flux were measured using two electronic–inductive flowmeters (MIK 5NA, Kobold Mesura). Temperature (TR2432, IFM), pH (Liquiline CM14, Endress+Hausser) and biogas production (FCI ST75) were continuously monitored. The biogas sparging flow rate was measured using a rotameter (PS Series, Tecfluid). The entire system was controlled by an Arduino based PLC (M–Duino 38R, Industrial Shields) connected to a PC for remote control and real time monitoring.

2.2   Slaughterhouse wastewater characteristics

The jet-loop AnFMBR was fed with raw wastewater from a pig slaughterhouse (Campofrio Frescos, Campofrio Food Group, Spain) collected from the homogenization pond, without any pre–treatment other than coarse screening and grit removal. The slaughterhouse wastewater was characterized by Chemical Oxygen Demand (COD) of 2970–6040 mg/L, with peak concentrations of up to 9715 mg/L, Total Organic Carbon (TOC) 1170–2130 mg/L, Oil and Grease (O&G) concentrations up to 960 mg/L, Total Nitrogen

(TN) of 258–414 mg/L, total suspended solids (TSS) of 1740–4200 mg/L, and volatile suspended solids (VSS) of 1585–3860 mg/L.

2.3 Wastewater and biogas analysis

Samples of wastewater influent, effluent and mixed liquor from the filtration tank were collected daily. TSS, VSS, COD and O&G were analysed according to Standard Methods for the Examination of Water and Wastewater (APHA 2001) [27]. TOC and TN were analysed using a TOC/TN analyser (TOC-VCPN Shimadzu, Japan), and biogas composition was weakly monitored using a mobile gas-meter device (Multitec 545) with CH_4, CO_2, H_2S and O_2 sensors.

2.4 Specific methanogenic activity of suspended and attached biomass

Anaerobic activity tests were carried out for samples of attached and suspended biomass collected from the upper part of the anaerobic filter column. After removing the first layer of carriers from the upper part of the anaerobic filter, 10 litres of carrier material, approximately 500 pieces, together with the mixed liquor entrapped in the interstitial void spaces, were taken. 20 pieces of the support media were carefully put into 2.1 L anaerobic culture bottles for the determination of the methanogenic activity of the attached biomass (ATb). Then permeate was added in each bottle to a total volume of 400 mL, just covering the carriers. Three samples were prepared in the same just to determine the total and volatile attached solids. These samples were vigorously stirred to release as much attached biomass as possible from the carriers. After taking out the suspension of detached biomass, 250 mL of permeate were added to the bottles and vigorously stirred again to detach the biomass that remained on the carriers, repeating this operation until the carriers looked clean. Attached biomass concentration was

8

expressed on the basis of bulk volume of the carriers. Samples of 400 mL of the suspension released during the sampling of carriers were used to determine the specific methanogenic activity of the suspended biomass (SSb).

Pet food was used as model substrate with an initial food to biomass ratio (S_0/X) of 0.5 g COD/g VSS. Blank samples of the attached and suspended biomass without substrate were prepared to subtract their biogas production from the fed samples. 1 g of $NaHCO_3$ was added to each culture bottle to provide alkalinity (1.5 g $CaCO_3$/L), and macro and micronutrients solutions were also supplied [28]. Each culture was prepared in triplicate. After removing O_2 with N_2, the bottles were incubated at 35ºC in a temperature–controlled room, being gently agitated in a Wheaton® roller culture device at 1.2 rpm.

Biogas production was monitored by a digital pressure sensor (PN 2569, IFM) throughout the assay, and methane concentration was analysed at the end of the tests. TSS and VSS concentration in each sample were also determined at the end of the methanogenic activity test.

2.5   Membrane performance

The effects of filtration flux, J, backwashing frequency (in terms of filtration cycle duration, t_c), backwashing flux, J_{bw}, and backwashing duration, t_{bw}, were studied on reversible fouling rate, critical flux, filtration and backwash resistances, compressibility, and irreversible fouling rate. Two types of experiments were carried out, short-term and mid-term. The short-term assays were composed of series of 8 cycles performed by stepwise increase of the flux, as in the flux-step method used for identifying the onset of the reversible fouling at the so-called critical flux. In the mid-term assays, the operating

2.5.1 Short-term filtration assays

Filtration and backwashing resistances, reversible fouling rate, critical flux, and

compressibility index were continuously monitored over one week by successive critical

flux determination, using eight fluxes: 11.6, 12.1, 13.7, 13.9, 14.2, 15.9, 16.2 and

17.9 L/m^2·h. To evaluate the effect of the backwashing intensity on the membrane

performance, three backwashing frequencies, t_c = 7 − 10.5 − 14 min, three backwashing

duration, t_{bw} = 20 − 30 − 40 s, and three backwashing strength, J_{bw}/J = 1.5 − 1.75 − 2.0,

were used.

A Box−Behnken experimental design was used to combine the three levels (high: +1,

intermediate: 0, and low: −1) of the three operating conditions (t_c, t_{bw} and J_{bw}/J), which

allowed the statistical analysis of the experimental results with a minimum number of

runs [29]. The Box-Behnken design allows to analyse the statistical relevance of the

effects of each variable and to obtain a response surface from the experimental results

using a quadratic polynomial model (Eq.1)

$$Y = b_0 + \sum b_i X_i + \sum b_{ii} X_i^2 + \sum b_{ij} X_i X_j \qquad (1)$$

where Y is the predicted response for the filtration resistance, the backwashing

resistance, the reversible fouling rate or the critical flux, b_0 is the corresponding intercept

coefficient, b_i is the linear effect coefficient of the operational parameter X_i, b_{ii} is the

quadratic effect coefficient of X_i, and b_{ij} is the interaction effect coefficient of the

operational parameters X_i and X_j.

The reversible fouling rate, $(dTMP/dt)_{rev}$, was determined by robust linear regression of the TMP profile using Huber's method to avoid that TMP outliers, associated with bubbling and other system fluctuations that contaminate the slope and intercept estimations of least squares regression. Huber's tuning constant was set to 1.345 according to 95% asymptotic efficiency rule [30]. The intercept of this linear regression, TMP_0, corresponds to the initial TMP, without the contribution of the reversible fouling, which has been removed by relaxation and backwashing.

The filtration resistance, R_f, in each critical flux series was determined from the slope of linear regression of TMP_0 versus J of the 8 cycles, by dividing it by the viscosity according to Darcy's Law. Likewise, the resistance to backwashing, R_{bw}, was determined from linear regression of backwash transmembrane pressure, TMP_{bw}, versus backwashing flux, J_{bw}.

Since the fouling layer is formed by soft sludge flocs easily deformable, the porosity and the packing structure of the cake layer will depend on applied pressure. Therefore, as the degree of cell deformation, the filtration resistance will be TMP dependent. The following empirical potential equation [31] was used to characterise the compressibility of the fouling layer, R_f:

$$R_f = r \cdot (TMP)^n \tag{2}$$

where, r is the resistance at unit TMP, and n is the compressibility index. The cake layer is considered uncompressible when n is zero, R_f independent of TMP, and increasing values of n represent increasing effect of TMP on filtration resistance, which provides a measure of the compression effects.

The critical flux was determined as the flux over which TMP slope exceeds an arbitrary value [32]. A $(dTMP/dt)_{rev}$ threshold of 1 mbar/min was chosen to decide when J_c was

reached [33]. For this, reversible fouling rates in the range $0.5 - 5$ mbar/min, was linearized versus the filtration flux and J_c was determined as the flux that makes $(dTMP/dt)_{rev}$ equal to the selected threshold.

2.5.2 Mid-term filtration assays: irreversible fouling rate determination

Three backwashing frequencies, t_c of 7.0, 10.5 and 14.0 min, filtration fluxes of 12.4 ± 0.1, 13.4 ± 0.1 and 14.5 ± 0.1 L/m$^2\cdot$h, and backwashing fluxes of 21.7 ± 0.1, 24.4 ± 0.2 and 26.5 ± 0.1 L/m$^2\cdot$h, were tested. The three levels of J, J_{bw} and t_c, were combined according to a Box–Behnken experimental design. The filtration cycles were composed of four stages: 40 s for relaxation between filtration and backwash, 30 s for backwash, 20 s for relaxation between backwash and filtration, and the remaining time until total cycle duration for filtration. After 7 hours of operation at the selected conditions, 8 cycles of 7.5 min with fluxes between 10.6 and 13.8 L/m$^2\cdot$h were performed for the determination of the critical flux.

The irreversible fouling rate was calculated as the increase in the hydraulic resistance over the net production of permeate per unit of membrane surface area, $(dR_0/dv)_{irr}$ (m^{-2}), being R_0 (m^{-1}) the resistance at the beginning of each filtration cycle, and v (m^3 m^{-2}) the net filtrated volume per unit of area. For this purpose, the increase of R_0 over time throughout each mid-term assay, $(dR_0/dt)_{irr}$, was divided by the net flux, J_{net}, according to Eqs. 3 and 4,

$$\left(\frac{dR_0}{dv}\right)_{irr} = \frac{(dR_0/dt)_{irr}}{J_{net}} \qquad (3)$$

$$J_{net} = \frac{J \cdot t_f - J_{bw} \cdot t_{bw}}{t_c} \qquad (4)$$

where, t_f is the duration of filtration, t_{bw} is the duration of backwash and t_c is the duration of the entire filtration cycle.

3 RESULTS AND DISCUSSION

3.1 Biological behaviour of the AnFMBR

3.1.1 Organic matter removal, biogas production and soluble microbial products

The jet-loop AnFMBR feed flow was set at 220 – 240 L/d, corresponding to an HRT of 19.5 – 21.3 h, independent of the net filtration flux due to the recirculation of the excess of permeate. The organic loading rate remained in the range of 3.5 – 7.4 kg COD/m³·d, depending mainly on the variation of influent COD. The removal efficiency remained between 92 and 97% with COD concentration in the effluent between 152 and 347 mg/L, free of oil and grease. León-Becerril *et al*. [18] treating cold meat industry wastewater in an anaerobic filter reached a stable OLR of 3.5 kg COD/m³·d achieving a lower COD removal efficiency, 84%, in spite of the use of a support media with a considerably higher specific surface area, 3600 m²/m³.

Accidentally the feeding tank of the pilot plant was filled with more concentrated wastewaters reaching OLRs of 10.9 kg COD/m³·d. The AnFMBR showed a great stability, an increase of feed COD up to 9715 mg/L for more than 48 h caused just an slightly increase in the effluent COD, from 187 to 394 mg/L, that immediately recovered the initial level when the feed COD and OLR returned to normal values. It is well known that hydraulic and organic shock loads cause detrimental effects on conventional anaerobic reactors, such as an increase of TSS in the effluent, flotation of suspended biomass or accumulation of volatile fatty acids. However, it has been reported that fixed-film

reactors shows higher stability and specially a better recovery when the shock loading was alleviated, which is attributed to the biomass entrapment [34].

The concentration of methane in the biogas was always higher than 74%, peaking at 82%. Biogas production was a little more stable than the applied organic loading rate, between 5.5 – 6.1 kg $COD_{CH4}/m^3 \cdot d$, possibly due to the buffer capacity of the anaerobic filter. The filter effect of the fixed bed allows capturing slowly biodegradable organic matter, without degrading it. So, when wastewater COD is in excess there is a net storage and, on the contrary, when OLR decreases, the stored COD is biodegraded, buffering its fluctuations.

The bioreactor operated without clogging problems, despite the wastewater TSS was up to 4200 mg TSS/L. This could be related to the jet-loop recirculation that allows keeping balanced biomass retention and sweeping of the filter, avoiding the clogging of the filter bed by biomass sloughing.

Polysaccharides (PS) and proteins (PN) concentrations in the permeate remained in the range of 29.2–37.9 mg PS/L and 4.6–9.0 mg PN/L. The concentration of humic substances (HS), was somewhat higher, 44.0–79.9 mg HS/L. The fouling capacity of HS is particularly important because they tightly bound to the cake layer by their phenolic and carboxylic functional groups, serving as nutrients for microbial growth [35]. These values were lower than the obtained in a batch filtration device (not published), 56.0 mg PS/L, 12.0 mg PN/L and 157.2 mg HS/L, by filtering a model suspension of slaughterhouse anaerobic sludge. The lower concentration of soluble microbial products is probably because the biomass of the jet-loop AnFMBR was subjected to lower shear stress conditions. It should be considered that the release of soluble microbial products is at the origin of the negative

effects of the shear forces in membrane fouling, leading to the formation of thinner but more compact gel layers, resulting in more serious fouling problems.

3.1.2 Biomass concentration and specific methanogenic activity

One of the difficulties in the study of anaerobic filters is the complexity of determining biomass quantity and activity [36]. Concentration and specific methanogenic activity (SMA) of attached and suspended biomass was determined from the sample taken from the top of the AF as described in 2.4 section.

It is worth noting that the bulk volume and effective porosity of the colonized material were different than the specifications of the clean material reported by the manufacturer, 75000 pieces/m^3 and 90%, respectively, corresponding to the so called "bagged material". The volume occupied by 20 pieces of the carrier material, approximately 400 mL, represents a bulk volume around 20 mL/piece, 40% higher than that of the bagged material. On the other hand, the layer of sludge retained by the carriers reduced the effective porosity of the colonized material, 64% according to the volume of permeate required to flood the carrier material in the culture bottles.

Attached and suspended biomass concentrations, at the beginning and at the end of the anaerobic activity test are given in **Table 1**, where the attached biomass concentration is expressed in relation to the bulk volume of the colonized carriers, in mg/L.

Table 1. Total and volatile suspended solids at the beginning and at the end of the methanogenic activity test.

	initial		Final	
	VSS (mg/L)	TSS (mg/L)	VSS (mg/L)	TSS (mg/L)
ATb*	14584 ± 1490	16385 ± 1714	15170 ± 1604	17040 ± 1695
SSb	3220 ± 117	3785 ± 133	3244 ± 211	3764 ± 233

(*) attached solids concentration are reported on the basis of the bulk volume of the carrier media, the attached solids by unit of area, in g/m^2, could be determined multiplying by $3.25 \cdot 10^{-3}$ the reported concentrations

It should be noted that an 82% of the biomass remains retained on the carriers, which reduces the concentration of the suspension in contact with the membrane, and therefore its fouling potential. The concentration of SSb within the anaerobic filter was in the range of the mixed liquor in the filtration tank, 3504±311 mg TSS/L. However, it should be highlighted that the SSb sample was taken from the upper part of the anaerobic filter column, where the mixed liquor from the filtration tank is returned to the anaerobic filter. The concentration of ATb was notably higher than the obtained in an anaerobic fixed-bed reactor specifically designed to allow the periodical withdrawal of biomass, using a support media consisted of PVC Raschig rings with a specific surface area of 230 m^2/m^3, in which a maximum biomass concentration of 14.0 g VS/m^2, equivalent to 3.2 kg VS/m^3, was reached [36].

The biomass concentrations at the end of the methanogenic activity tests were only slightly higher than the initial ones. However, an important difference was observed in the ATb cultures. At the end of the test most of the biomass was in suspension and the carriers were almost clean. In fact, the biomass that remained attached, analysed after

taking out the suspension and stirring vigorously the carriers in 250 mL of permeate, was lesser than 4% of the total. The biomass was loosely bound to the carriers and solids detachment was appreciable after a few hours, despite the low rotational speed of the roller device, only 1.2 rpm. Another sign of the weakness of the biomass attachment was observed accidentally after a slow leaking out of the anaerobic filter. A quick refilling of the AF column caused an increase in TSS in the filtration tank, up to 8407 mg/L, due to the release of part of the biomass retained in the interstices of the support media.

Figure 2 shows the conversion of organic matter into methane through time by the attached and suspended biomass. The substrate was almost completely digested in 21 days. Methane production was not uniform through time, so three periods can be distinguished: (a) methanogenesis of readily biodegradable organic matter, S_s, (b) hydrolysis of slowly biodegradable organic matter, X_s, and (c) endogenous decay of heterotrophic biomass, X_H, schematically represented on the Figure 2. No significant differences were observed between attached and suspended biomass in the periods (a) and (c), however, it can be observed that the attached biomass had a higher hydrolytic capacity than the suspended biomass. Alves *et al*. [36] checked that both acetoclastic and hydrogenotrophic methanogenic of attached biomass were very close to those of the suspended biomass, confirming the dual role of the carrier material in the biomass retention: attachment and filtration of the biomass in suspension. Table 2 shows the length and the specific methanogenic activity during the three periods of both sludges. Ho and Sung [37] determined the microbial activity of the biomass suspended in the bioreactor and attached on the membrane surface of a side-stream AnMBR. In this work, lower SMAs were obtained, 0.1 – 0.17 g COD_{CH4}/g VSS·d, and a gradual decrease of SMA of the attached biomass, directly related to shear force of the cross flow, was observed.

However, the harsh hydrodynamic conditions of the side-stream AnMBRs, are not comparable to those of the jet–loop AnFMBR. The superficial velocities of the sludge, 0.002 m/s, and of the gas, 0.02 m/s, in this work were one-two order of magnitude lower than the used in side-stream tubular membranes operated with gas sparging, 0.51 m/s and 0.15 m/s, for sludge and gas respectively [38]. In fact, the rate of hydrolysis of slowly biodegradable substrate by the attached biomass was faster than that of the suspended biomass. The slowly biodegradable organic matter was almost digested by the attached biomass in half the time taken by the suspended one. These results showed that the differences in biomass location can impact the development of different microbial communities in the AnFMBR. The longer sludge age of the attached biomass likely favours the development of methanogenic bacteria with slower growth rates, which would justify the higher methanogenic activity of the attached biomass, but not its higher hydrolytic activity. Harb *et al.* [39] suggested that an AnMBR with suspended biomass was likely able to overcome fermentation digestion steps more efficiently than an attached biomass AnMBR system. However, it should be considered that the particulate organic matter in the jet-loop AnFMBR is physically entrapped by the biomass retained by the carrier material, justifying that the so-called attached biomass had a higher hydrolytic capacity than the suspended one.

A treatment capacity of 6.40 kg COD/m^3·d, slightly higher than the observed in the continuous operation of the jet-loop AnFMBR, was calculated from the concentration and SMA of the attached and suspended biomass. According to the concentration and methanogenic activity of both types of biomass, it can be concluded that only a 16% of the biological activity of the jet-loop AnFMBR corresponds to the suspended biomass.

Therefore, it can be expected that an increase of the sludge withdrawal, aimed to reduce membrane fouling, would only cause a small decrease in its treatment capacity.
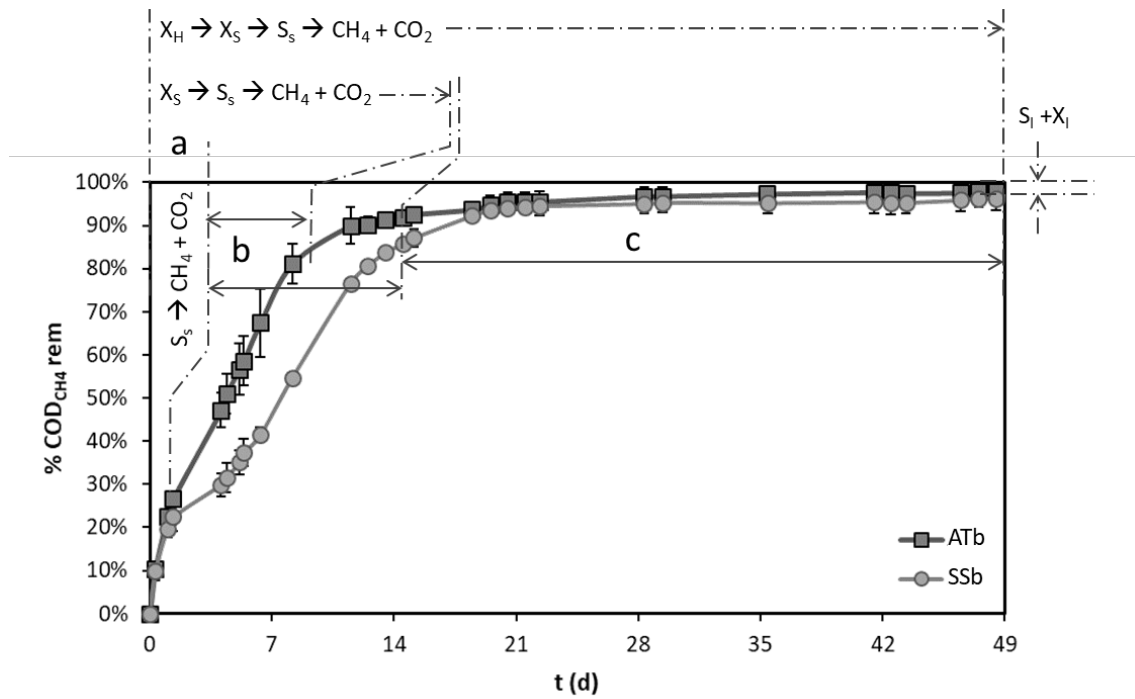

Figure 2. COD removal over time by attached biomass (ATb) and suspended biomass (SSb). S_s: easily biodegradable substrate; S_I: inert soluble organic matter; X_s: slowly biodegradable biomass; X_H: heterotrophic biomass; X_I: inert suspended organic matter.

Table 2. Specific methanogenic activity of the attached and suspended biomass during the three periods (a) readily biodegradable substrate methanogenesis, (b) slowly biodegradable substrate hydrolysis and (c) endogenous decay of biomass.

Period	(a)		(b)		(c)	
	t_i – t_f (d)	SMA* (R^2)	t_i – t_f (d)	SMA (R^2)	t_i – t_f (d)	SMA (R^2)
ATb	0.0 – 1.3	0.388 (0.976)	4.1 – 8.2	0.156 (0.997)	13.5 – 53.5	0.003 (0.828)
SSb	0.0 – 1.3	0.357 (0.961)	4.1 – 19.5	0.129 (0.991)	22.3 – 56.5	0.005 (0.961)

(*) g COD$_{CH4}$/g VSS·d

3.2 Filtration performance

3.2.1 Short–term assays: effect of backwashing intensity on hydraulic resistances

Throughout the short–term assays the hydraulic resistances of the membrane slowly increased as consequence of the irreversible fouling. The filtration resistance increased $0.015·10^{12}$ m^{-1}/d, equivalent to 0.49 mbar/d for an average flux of 14.8 L/m^2·h, as the increase in backwashing resistance was $0.024·10^{12}$ m^{-1}/d. This increase in filtration resistance was notably lower than the obtained by Wang *et al.* [21], $0.110·10^{12}$ m^{-1}/d, in an anaerobic hybrid membrane bioreactor, combining a fixed bed of granular activated carbon and a stainless-steel mesh used as filter, treating low-strength synthetic wastewater. A statistical analysis of the relationship between the resistances and backwash intensity was performed, aiming to determine which variables, backwash interval (duration of the cycle, t_c), backwash duration (t_{bw}) or backwash strength (J_{bw}/J), were more significant in the experimental range. The standardized effects of each

variable and their interactions are represented in a modified Pareto diagram (**Figure 3**), where the vertical line permits to judge which operating conditions are statistically significant, with a confidence level of 95%. The bars that exceed the reference line correspond to variables or interactions whose effects on the response variable (resistance, critical flux of reversible fouling rate) are potentially important. A positive sign (+) bar label indicates that the response increased with the variable within the range studied; whereas a minus sign (−) bar label indicates that the response decreased when the variable increased.

The three variables, t_c, t_{bw} and J_{bw}/J, had a relevant standardized effect on the filtration resistance (**Figure 3**.a). t_c caused an increase in R_f whereas t_{bw} and J_{bw}/J led to its reduction. The quadratic effect of the duration of the filtration cycle, t_c^2, was also statistically significant, in this case with a negative sign, meaning that as the duration of the filtration cycle increases its positive effect decreases. Regarding the backwashing resistance, t_c and specially J_{bw}/J had a standardized effect notably higher than t_{bw}, whose effect was not statistically relevant. The duration of backwashing only had statistically significant effects through the interactions, $t_c \cdot t_{bw}$ and $t_{bw} \cdot J_{bw}/J$, which means that R_f only is affected by t_{bw} when the duration of the filtration cycle and/or backwash strength are high.

It is worth noting that the signs of standardized effects of the variables with significant effect on R_f and R_{bw} are opposite. This means that the increase of backwash frequency and/or backwash strength, reduces the global resistance, but could have negative effects on the backwashing resistance.
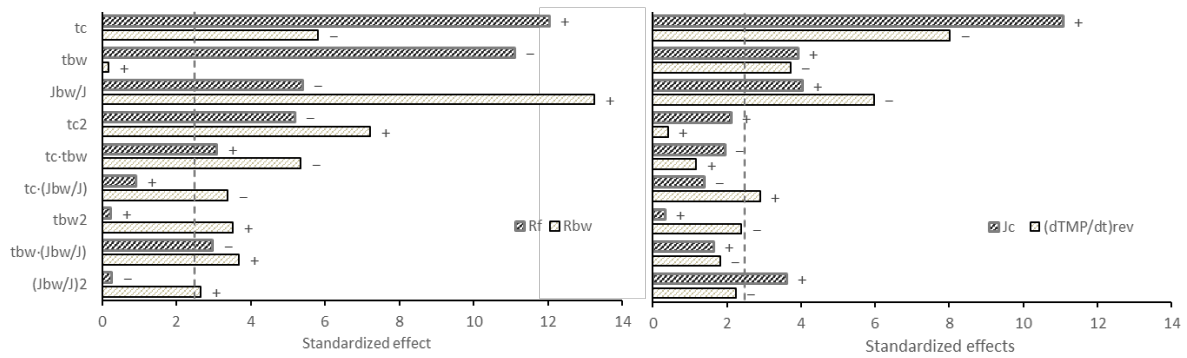
Figure 3. Standardized effect of the duration of filtration cycle, t_c, backwash duration, t_{bw} and strength (J_{bw}/J) and their interactions on (a) filtration resistance, R_f, and backwash resistance, R_{bw}, and (b) critical flux, J_c and reversible fouling rate (dTMP/dt)$_{rev}$ for 15.9 L/m^2·h.

Table 3 shows the coefficients of the polynomic model (Eq. 1) and the coefficients of correlation (R-squared), resulting from the statistical treatment of the results obtained for both resistances. Between brackets are written the significant standardized effects and between squared brackets the standardized effects of non-significant variables. The R_f and R_{bw} estimated by the model are represented versus the experimental resistances (**Figure 4**) from the 72 short–term assays performed in the current experiment. It can be observed that the predicted and experimental data of R_f and R_{bw} are well adjusted to the 1:1 dashed line, even despite the experimental range was very narrow, $1.27 - 1.48 \cdot 10^{12}$ m^{-1} for the backwash resistance and $1.33 - 1.64 \cdot 10^{12}$ m^{-1} for the total resistance.

Table 3. Model coefficients for the filtration and backwashing resistance estimation from short-term assays (the significant standardized effects are showed under brackets and the non-statistically significant effects are showed under squared brackets).

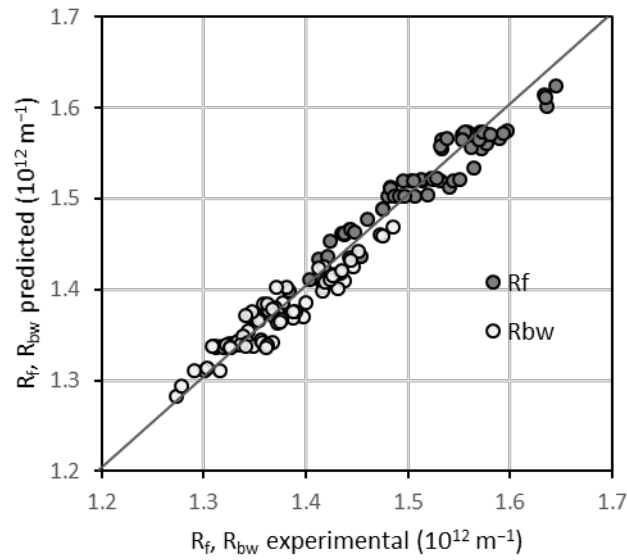|	Intercept	t_c	t_{bw}	J_{bw}/J	t_c^2	$t_c \cdot t_{bw}$	$t_c \cdot$ (J_{bw}/J)	t_{bw}^2	$t_{bw} \cdot$ (J_{bw}/J)	$(J_{bw}/J)^2$	R^2 corr
R_f	1.2015	2.7707	0.0016	0.1465	−9.9936	0.033	0.3772	$1.25 \cdot 10^{-5}$	−0.0075	−0.024	0.986
		(12.04)	(11.1)	(5.39)	(5.18)	(3.09)	[0.91]	[0.24]	(2.97)	[0.26]	
R_{bw}	1.897	−0.6557	−0.0124	−0.4825	8.7444	−0.0364	−0.9086	$1.45 \cdot 10^{-4}$	0.0058	0.176	0.985
		(5.82)	[0.18]	(13.24)	(7.22)	(5.35)	(3.37)	(3.52)	(3.67)	(2.64)	

Figure 4. Estimated result fitted by the model related to experimental results for filtration and backwash resistance.
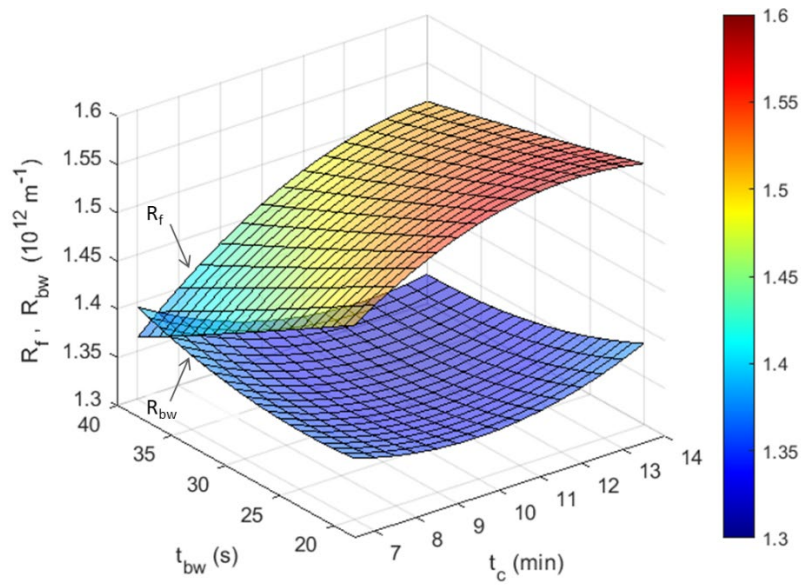
Figure 5. Three–dimensional response surface of the total and backwash resistance vs cycle and backwash duration corresponding to the intermediate backwashing strength, J_{bw}/J of 1.75.

Figure 5 represents the three–dimensional response surfaces of the total and backwash resistances versus the frequency and duration of backwashing, both for a backwashing strength, $J_{bw}/J = 1.75$. It can be observed that the highest filtration resistance was obtained at the longest filtration cycles and the shortest backwashing time. Backwash efficiency in R_f reduction, was notably higher for $t_c = 7$ min than for $t_c = 14$ min. The convexity of both surfaces is opposite, according to standardized effects, showing that the conditions that controlled total resistance had a small but significant negative effect on the internal resistance. Therefore, this potentially negative effect, possibly due to the deterioration of the permeate quality in the permeate vessel [40], should be considered for an effective fouling control in long term operation of membrane bioreactors.

3.2.2 Reversible fouling rate, critical flux and compressibility index from short–term assays

Figure 3.b shows the standardized effects of the backwash intensity on critical flux and on the reversible fouling rate of the cycles conducted at a flux of 15.9 L/m^2·h. As expected, those variables that caused a decrease of the reversible fouling caused an increase of the critical flux, and therefore the signs of the standardized effects on $(dTMP/dt)_{rev}$ and J_c are opposite.

In the present work the most influential variable on $(dTMP/dt)_{rev}$, was surprisingly t_c. The duration of the filtration cycle does not alter the balance between convective drag to the membrane and back transport due to gas sparging causing the reversible fouling. However, t_c could modify TMP slope by the effect of the progressive compression of the fouling layer. It takes time for the fouling layer to be compressed, so specially at the beginning of filtration TMP increase is not only due to the attachment of new materials but also to the compression of the pre-existing fouling layer [41]. This TMP rise, normally attributed to reversible fouling, decreases with time and therefore, as t_c increases TMP slope was lower.

The compressibility index of the fouling layer, n, was found to be independent of t_{bw} and J_{bw}/J. However, both t_c and t_c^2 had significant effects on the compressibility index, especially between 10.5 min to 14 min, increasing from 0.376±0.057 to 0.481±0.021. This result could be explained because the compression is time and TMP dependent. On the one hand, even at constant pressure, it takes time for the fouling layer to be rearranged to a less porous structure. Therefore, the longer filtration duration, the higher compressibility index is obtained. On the other hand, it should be considered that the

compressibility index is determined from the TMP at the beginning of each filtration cycle. Therefore, as TMP increases throughout the filtration, the fouling layer compression also increases for longer filtration duration.

Critical fluxes remained between 14.52 and 15.77 $L/m^2 \cdot h$. Backwashing duration and strength and specially the longer duration of the filtration cycle caused an increase of critical flux (**Figure 3**.b). **Figure 6** shows the response surfaces of critical flux versus t_c and t_{bw} for two backwashing strengths 1.5 and 2.0. The increase in critical flux with t_c is also directly related to the compression that reduces the TMP slope when t_c is longer, what justifies the higher flux required to reach the threshold of dTMP/dt of 1 mbar/min. The critical flux increased as t_{bw} did, especially for J_{bw}/J of 2.0 and the shorter t_c. The effect of backwashing intensity on the critical flux suggests that a strong backwashing leads to an increase of the effective area of the membrane and resulting in higher scouring efficiency, which raises the critical flux.
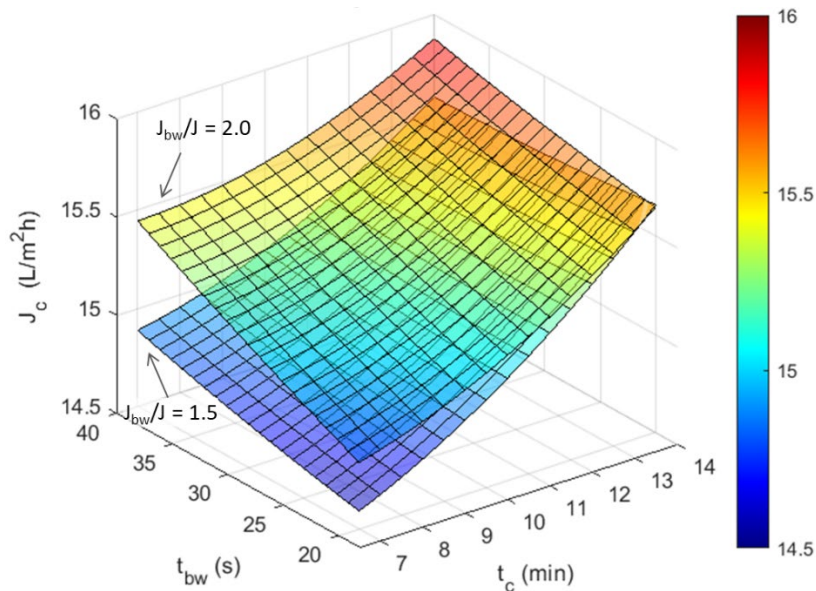

Figure 6. Critical flux vs the duration of filtration cycle and backwash for two backwashing strengths, J_{bw}/J = 1.5 and 2.0.

Finally, a summary of the effects of backwashing scenarios on the filtration and backwash resistances, critical flux, reversible fouling rate and compressibility index observed in the short−term assays is presented in **Table 4**, where a positive sign means that the value of the variable increases with the correspondent operational parameter.

Table 4. Qualitative effects of the backwashing intensity on the filtration process in the jet-loop AnFMBR observed in the short−term assays.

	R_f	R_{bw}	J_c	$(dTMP/dt)_{rev}$	n
t_c	$(+)^-$	$(-)$	$(+)$	$(-)$	$(+)^+$
t_{bw}	$(-)$	$(0)^+$	$(+)$	$(-)$	w.e.
J_{bw}/J	$(-)$	$(+)^+$	$(+)^+$	$(-)$	w.e.

Superindex: quadratic effect: $(+)^+$ positive effect increases as the variable increases, $(+)^-$ positive effect decreases as the variable increases, $(0)^+$ positive effect only at the highest levels. w.e.: without effect.

3.2.3 Reversible and irreversible fouling rates vs J, J_{bw} and t_c from mid−term assays

The filtration fluxes used in the mid-term assays were in the range of 12.4−14.5 L/m^2·h, higher than the applied in most AnMBR studies, generally below 12 L/m^2·h [42,43]. These fluxes were possible thanks to the capacity of the jet-loop AnFMBR to keep the concentration of suspended solids in the filtration tank low, 3504±311 mg TSS/L. Jensen *et al*. [44] treated slaughterhouse wastewater using a completely mixed AnMBR. With an estimated biomass concentration of 40 g TSS/L the membrane could only operate sustainably at flux lower than 5 L/m^2·h, despite using a SGD of 2.26 Nm^3/m^2·h. In this study it was necessary to reduce the biomass concentration to 30 g TSS/L to reach a filtration flux of 7 L/m^2·h, similar to the previously achieved in other AnMBRs treating slaughterhouse wastewater [26,45].

The analysis of the standardized effects of filtration flux, duration of the filtration cycle and backwash flux on $(dTMP/dt)_{rev}$ (**Table 5**) showed that J, with a positive effect, and t_c, with a negative effect, were the most influential variables on reversible fouling rate in the mid-term assays. Just as in the short-term assays, J_{bw} also had a negative effect through the quadratic contribution, i.e. for high J_{bw}. The standardized effects of J, t_c and J_{bw} on $(dR_0/dv)_{irr}$ revealed that the effect of backwashing flux in controlling $(dR_0/dv)_{irr}$ was not statistically significant. However, the filtration flux, the filtration cycle duration, and their interaction, $J \cdot t_c$, contributed positively to the irreversible fouling of the membrane. This is because high filtration flux, and consequently high TMP, and long filtration duration results in a more compact fouling layer, harder to remove by backwashing.. It is worth noting that the sign of the effects of t_c on reversible and irreversible fouling are opposite, what means that the increase in t_c diminishes TMP slope but contributes to consolidate the fouling layer. In addition, it is important to emphasize that the approaches that might diminish the reversible fouling, in this case longer t_c, are not always effective for irreversible fouling control, could even have the contrary effect.

Table 5. Model coefficients for reversible and irreversible fouling rate estimation, and standardized effects from mid-term assays (the significant are showed under brackets and non–statistically significant under squared brackets).

	Intercept	t_c	J	J_{bw}	t_c^2	$t_c \cdot J$	$t_c \cdot J_{bw}$	J^2	$J \cdot J_{bw}$	J_{bw}^2	R^2 corr
$(dTMP/dt)_{rev}$	−30.7429	1.8864	−15.737	9.5946	−0.0054	−0.0959	−0.0304	0.7689	−0.0665	−0.1720	0.975
		(−4.48)	(+12.14)	[+1.07]	[−0.23]	[−1.25]	[−0.87]	(+2.86)	[−0.59]	(−3.36)	
$(dR_0/dv)_{irr}$	72.518	−2.9677	−14.236	2.2421	0.00498	0.2102	0.0113	0.5485	−0.0352	−0.0404	0.905
		(+4.58)	(+8.88)	[−0.62]	[+0.21]	(+3.00)	[+0.36]	(+2.04)	[−0.24]	[−0.8]	

The quadratic model, Eq. 1, correlated reasonably well $(dTMP/dt)_{rev}$ ($R^2 = 0.975$) and $(dR_0/dv)_{irr}$ ($R^2 = 0.905$) with the filtration and backwashing fluxes and the duration of the filtration cycle. This is particularly relevant in the case of the irreversible fouling rate, despite its lower coefficient of correlation, taking into account the challenge of determining $(dR_0/dv)_{irr}$ by mid-term assays, particularly for the lowest irreversible fouling rates. **Figure 7** represents the estimated reversible and irreversible fouling rates versus the experimentally obtained in the mid–term assays and compares them with the 1:1 reference line (dashed line). Negative values of $(dR_0/dv)_{irr}$, unsustainable in long-term operation of the system, reveal that the interval of 7 hours used in the mid-term assays, is insufficient to accurately determine low $(dR_0/dt)_{irr}$. In fact, small pressure fluctuations can be misinterpreted as negative irreversible fouling rate, for instance, the represented $(dR_0/dv)_{irr}$ around $-0.3 \cdot 10^{12}$ m^{-2}, corresponds to a TMP decrease lower than 1 mbar throughout 7 h. Those runs were not excluded from the statistical analysis since, even negative values of $(dR_0/dt)_{irr}$, reflects the trend of the irreversible fouling rate.
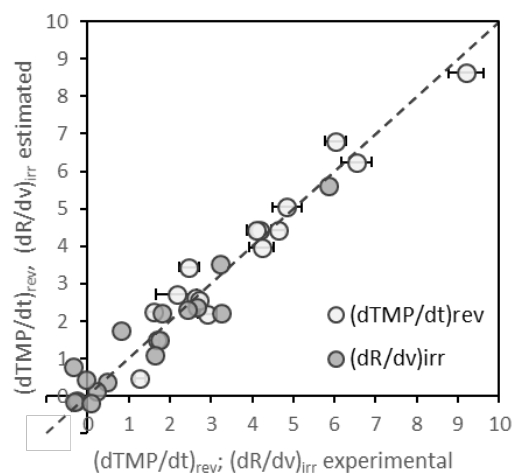

Figure 7. Estimated vs experimental reversible and irreversible fouling rates, in mbar/min and 10^{12} m^{-2}, respectively.
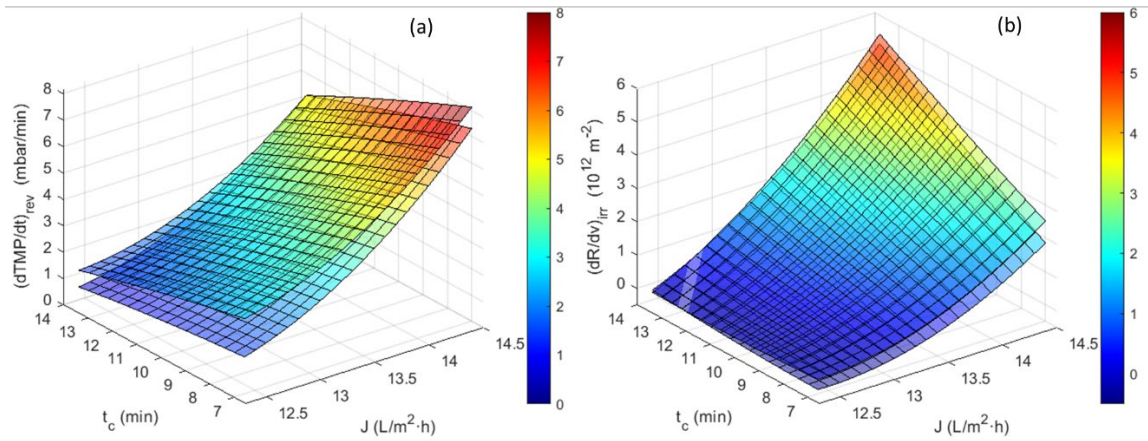
Figure 8. Three–dimensional response surface of the (a) reversible and (b) irreversible fouling rates vs filtration flux and cycle duration, for backwashing fluxes of 21.7 L/m^2·h and 26.5 L/m^2·h.

The response surfaces of the reversible and irreversible fouling rates (**Figure 8**) show that the most important factor affecting them was the filtration flux. The reversible fouling rate (**Figure 8**.a) was slightly affected by t_c for the lowest J, and therefore lower pressure, initial TMP of 65.4±2.0 mbar. However, $(dTMP/dt)_{rev}$ decreases in 3 mbar/min for the highest J, initial TMP of 100.5±3.9 mbar, for which the effect of the compression was also higher. The irreversible fouling rate (**Figure 8**.b) was practically null for a filtration flux of 12.4 L/m^2·h, regardless of the duration of the filtration cycle and the backwashing flux. $(dR_0/dv)_{irr}$ increased with the flux and the duration of the filtration cycle, exceeding 5 10^{12} m^{-2} for J = 14.5 L/m^2·h and t_c = 14 min. The effect of J on $(dR_0/dv)_{irr}$ for the lowest t_c, 7 min, for the same flux was clearly lower reaching just 2.5 10^{12} m^{-2}. **Figure 8**.b shows that extending t_c from 7 to 14 min, for J = 14.5 L/m^2·h, doubled the irreversible fouling rate. In a previous work with an internal gas-lift AnFMBR, in which the filtration chamber was inside the anaerobic filter, an increase in t_c from 10 and 30 min resulted in a $(dR_0/dv)_{irr}$ 232% higher [22]. Raffin *et al*. [46] proved that at low flux, shortening backwash interval contributes little to diminish the CIP interval and that backwash interval become

increasingly significant as flux increases. By comparing the effect of t_c in **Figure 8**.a and **Figure 8**.b it is important to highlight that, despite $(dTMP/dt)_{rev}$ decreases with the cycle duration, $(dR_0/dv)_{irr}$ increases significantly.

A slight effect of the backwash flux on both fouling rates was observed. According to the standardized effects given in **Table 5**, only J_{bw}^2 had a statistically significant effect on $(dTMP/dt)_{rev}$. The surfaces response (**Figure 8**) shows that when J_{bw} changes from 21.7 to 26.5 L/m²·h the differences in $(dTMP/dt)_{rev}$, were lower than 1 mbar/min, while the differences in $(dR_0/dv)_{irr}$ were hardly appreciable. These results disagree with those obtained with the conventional flux step method by Zsirai *et al*. [47]. In this work the reversible fouling rates were hardly affected by flux and duration of backwash.

A widely accepted recommendation to reduce irreversible fouling is keeping the filtration flux below the critical flux [48]. However, it has been proved that it is possible to keep under control $(dR_0/dv)_{irr}$ even at a supracritical flux, with $(dTMP/dt)_{rev}$ up to 5 mbar/min, by increasing the backwash frequency to avoid the consolidation of the fouling. **Figure 9** shows that for $(dTMP/dt)_{rev}$ around 4.1–4.8 mbar/min, $(dR_0/dv)_{irr}$ could vary between −0.3 and 3.2 m^{-2}, depending mainly on the duration of the filtration cycle.
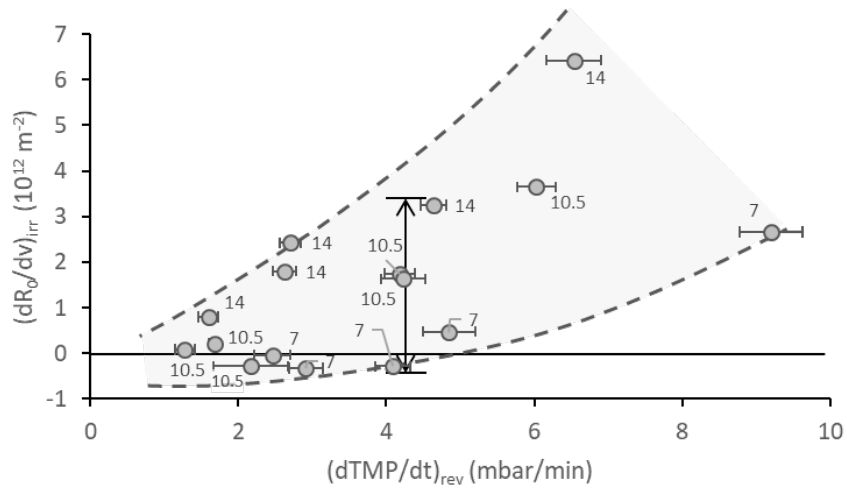
Figure 9. Irreversible vs reversible fouling rate. Data labels indicate the duration of the filtration cycle in minutes.

Figure 10 schematically represents the transformation of reversible to irreversible fouling, with emphasis on the effect of time, pressure and compression on the consolidation process. Reversible fouling is determined by the balance between particle transport towards the membrane coupled to filtration flux, and particle back-transport, coupled to gas sparging. The materials deposited on the membrane surface are easily detachable if TMP and time of compression are low. However, although the irreversible fouling rate was low, as TMP and compression time increase the consolidation of the fouling layer results in irreversible fouling. In this process the biomass concentration plays a double role. Sludge viscosity increases and bubble induced turbulence decreases as biomass concentration increases. Sludge concentration is also related with compression since thick reversible fouling layer are exposed to higher transmembrane pressures.
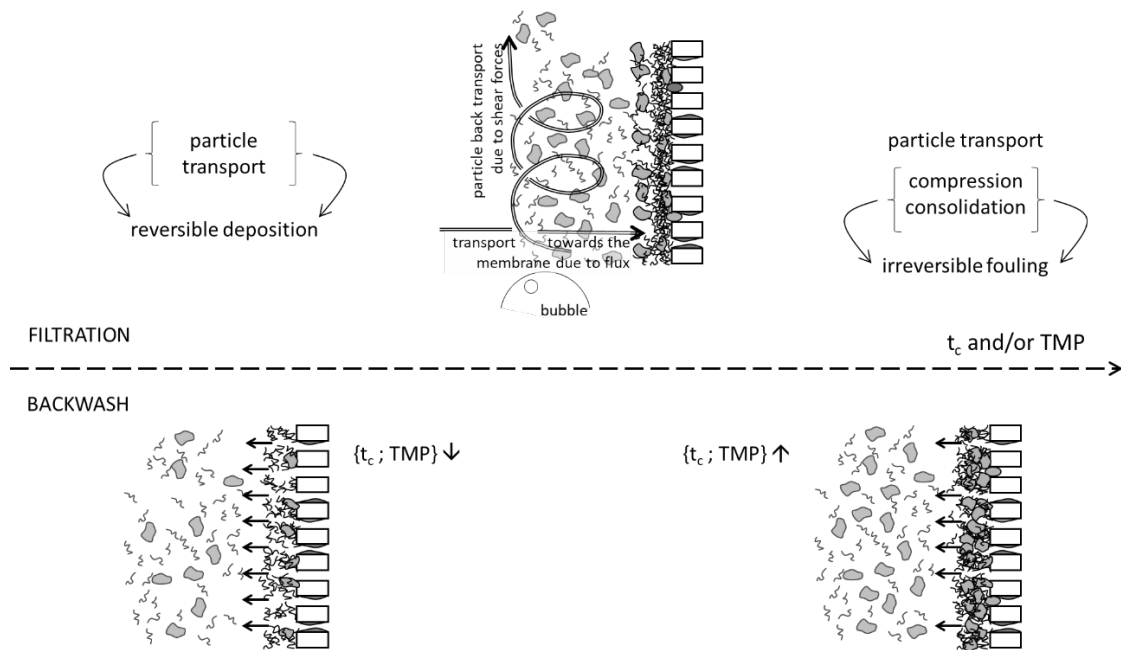
Figure 10. Schematic representation of the time and TMP dependence of the compression process that consolidate the reversible fouling

3.2.4 Critical flux and compressibility index evolution

Neither the critical flux nor the compressibility index showed any statistically significant relationship with t_c, J and/or J_{bw} used in the mid-term assays. It should be remembered that in mid-term assays, unlike the short-term assays, J_c and n were determined after each assay in the same flux steps and backwashing conditions, $J = 10.6 - 13.8$ L/m^2·h $t_c = 7.5$ min, $t_{bw} = 30$ s and $J_{bw}/J = 1.75$. The critical flux slightly decreased from 12.0 to 11.1 L/m^2·h due to the irreversible membrane fouling, still clearly above the values for the aforementioned AnMBRs treating slaughterhouse wastewaters. The compressibility index of the fouling layer remained between 0.31 and 0.43, without observing any correlation with the irreversible fouling behaviour. n was practically the same than the determined in those short-term assays performed with $t_c = 7$ min, 0.38±0.06.

4   CONCLUSIONS

A novel anaerobic membrane bioreactor, jet-loop anaerobic filter membrane bioreactor (AnFMBR), composed of a downflow anaerobic filter and a membrane tank, that takes advantage of the gas-lift effect caused by the gas sparging, has been studied at pilot-scale for raw slaughterhouse wastewater treatment.

The results have showed that organic matter removal efficiency remained between 92 and 97% with a treatment capacity of 5.5 – 6.1 kg COD/m^3·d. Approximately 82% of the active biomass was loosely attached to the carrier material, with an specific methanogenic activity of 0.388 g COD$_{CH4}$/g VSS·d and a hydrolytic capacity higher than that of the suspended biomass. The jet-loop AnMBR was very stable against sharply increases of the OLR, due to its high biomass retention capacity.

The filtration stage was studied by means of short-term assays, uninterrupted series of critical flux experiments, and mid-term assays, in which the operating conditions were the same for 7 h. In the short-term assays, the effect of different backwashing scenarios on the filtration and backwash resistances, reversible fouling rate, critical flux and compressibility index, were studied. In the mid-term assays, the evaluation of the irreversible fouling rate was included. Box-Behnken experimental designs were used for the statistical analysis of the relevance of the effects of the operating conditions on filtration performance and to obtain the multivariable response surfaces.

The increase in frequency and strength of backwashing reduced filtration resistance. Nevertheless, those changes caused a slight increase in internal membrane fouling. The duration of the filtration stage increased the compression and consolidation of the fouling layer, resulting in an increase in irreversible fouling rate.

The main factor affecting the reversible and the irreversible fouling rates was the filtration flux. $(dTMP/dt)_{rev}$ and $(dR_0/dv)_{irr}$ were affected differently by the duration of the filtration cycle. $(dTMP/dt)_{rev}$ diminished with time, however, $(dR_0/dv)_{irr}$ underwent an important rise, specially at high filtration flux. For roughly the same $(dTMP/dt)_{rev}$, $4.1 - 4.8$ mbar/min, $(dR_0/dv)_{irr}$ varied between -0.3 and $3.2 \cdot 10^{12}$ m^{-2} depending on the duration of the filtration cycle.

References

[1]   A. Ferreira, P. Marques, B. Ribeiro, P. Assemany, H.V. de Mendonça, A. Barata, A.C. Oliveira, A. Reis, H.M. Pinheiro, L. Gouveia, Combining biotechnology with circular bioeconomy: From poultry, swine, cattle, brewery, dairy and urban wastewaters to biohydrogen, Environ. Res. 164 (2018) 32–38. https://doi.org/10.1016/j.envres.2018.02.007.

[2]   R.A. Hamza, O.T. Iorhemen, J.H. Tay, Advances in biological systems for the treatment of high-strength wastewater, J. Water Process Eng. 10 (2016) 128– 142. https://doi.org/10.1016/j.jwpe.2016.02.008.

[3]   R.K. Dereli, M.E. Ersahin, H. Ozgun, I. Ozturk, D. Jeison, F. van der Zee, J.B. van Lier, Potentials of anaerobic membrane bioreactors to overcome treatment limitations induced by industrial wastewaters, Bioresour. Technol. 122 (2012) 160–170. https://doi.org/10.1016/j.biotech.2012.05.139.

[4]   R. Rajagopal, M.R. Choudhury, N. Anwar, B. Goyette, M.S. Rahaman, Influence of pre-hydrolysis on sewage treatment in an Up-Flow Anaerobic Sludge BLANKET (UASB) reactor: A review, Water (Switzerland). 11 (2019) 3–7. https://doi.org/10.3390/w11020372.

[5]   R.C. Leitão, A.C. Van Haandel, G. Zeeman, G. Lettinga, The effects of operational and environmental variations on anaerobic wastewater treatment systems: A review, Bioresour. Technol. 97 (2006) 1105–1118. https://doi.org/10.1016/j.biortech.2004.12.007.

[6]   C.S. Hwu, G. Lettinga, Acute toxicity of oleate to acetate-utilizing methanogens in mesophilic and thermophilic anaerobic sludges, Enzyme Microb. Technol. 21 (1997) 297–301. https://doi.org/10.1016/S0141-0229(97)00050-1.

[7]   J. Jeganathan, G. Nakhla, A. Bassi, Long-term performance of high-rate anaerobic reactors for the treatment of oily wastewater, Environ. Sci. Technol. 40 (2006) 6466–6472. https://doi.org/10.1021/es061071m.

[8]   M.M. Alves, M.A. Pereira, D.Z. Sousa, A.J. Cavaleiro, M. Picavet, H. Smidt, A.J.M. Stams, Waste lipids to energy: how to optimize methane production from long-chain fatty acids (LCFA), Microb. Biotechnol. 2 (2009) 538–550. https://doi.org/10.1111/j.1751-7915.2009.00100.x.

[9]   S. Singh, J.M. Rinta-Kanto, R. Kettunen, H. Tolvanen, P. Lens, G. Collins, M. Kokko, J. Rintala, Anaerobic treatment of LCFA-containing synthetic dairy wastewater at 20 °C: Process performance and microbial community dynamics, Sci. Total Environ. 691 (2019) 960–968. https://doi.org/10.1016/j.scitotenv.2019.07.136.

[10]   C. Ramos, A. García, V. Diez, Performance of an AnMBR pilot plant treating high-strength lipid wastewater: biological and filtration processes., Water Res. 67

(2014) 203–15. https://doi.org/10.1016/j.watres.2014.09.021.

[11]   M. Kamali, M.E. Costa, T.M. Aminabhavi, I. Capela, Sustainability of treatment

       technologies for industrial biowastes effluents, Chem. Eng. J. 370 (2019) 1511–

       1521. https://doi.org/10.1016/j.cej.2019.04.010.

[12]   M. Kamali, D.P. Suhas, M.E. Costa, I. Capela, T.M. Aminabhavi, Sustainability

       considerations in membrane-based technologies for industrial effluents

       treatment, Chem. Eng. J. 368 (2019) 474–494.

       https://doi.org/10.1016/j.cej.2019.02.075.

[13]   J.C. Young, Factors affecting the design and performance of upflow anaerobic

       filters, Water Sci. Technol. 24 (1991) 133–155.

       https://doi.org/10.2166/wst.1991.0222.

[14]   M. Farhadian, M. Borghei, V. V. Umrania, Treatment of beet sugar wastewater by

       UAFB bioprocess, Bioresour. Technol. 98 (2007) 3080–3083.

       https://doi.org/10.1016/j.biortech.2006.10.039.

[15]   H. Gannoun, H. Bouallagui, A. Okbi, S. Sayadi, M. Hamdi, Mesophilic and

       thermophilic anaerobic digestion of biologically pretreated abattoir wastewaters

       in an upflow anaerobic filter, J. Hazard. Mater. 170 (2009) 263–271.

       https://doi.org/10.1016/j.jhazmat.2009.04.111.

[16]   W.P. Tritt, H. Kang, Slaughterhouse wastewater treatment in a bamboo ring

       anaerobic fixed-bed reactor, Environ. Eng. Res. 23 (2018) 70–75.

       https://doi.org/10.4491/eer.2017.040.

[17]   F. Omil, J.M. Garrido, B. Arrojo, R. Méndez, Anaerobic filter reactor performance

       for the treatment of complex dairy wastewater at industrial scale, Water Res. 37

       (2003) 4099–4108. https://doi.org/10.1016/S0043-1354(03)00346-4.

[18]   E. León-Becerril, J.E. García-Camacho, J. Del Real-Olvera, A. López-López, Performance of an upflow anaerobic filter in the treatment of cold meat industry wastewater, Process Saf. Environ. Prot. 102 (2016) 385–391. https://doi.org/10.1016/j.psep.2016.04.016.

[19]   Y.Q. Tang, Y. Fujimura, T. Shigematsu, S. Morimura, K. Kida, Anaerobic treatment performance and microbial population of thermophilic upflow anaerobic filter reactor treating awamori distillery wastewater, J. Biosci. Bioeng. 104 (2007) 281–287. https://doi.org/10.1263/jbb.104.281.

[20]   J. V. Thanikal, M. Torrijos, F. Habouzit, R. Moletta, Treatment of distillery vinasse in a high rate anaerobic reactor using low density polyethylene supports, Water Sci. Technol. 56 (2007) 17–24. https://doi.org/10.2166/wst.2007.467.

[21]   Y.K. Wang, X.R. Pan, G.P. Sheng, W.W. Li, B.J. Shi, H.Q. Yu, Development of an energy-saving anaerobic hybrid membrane bioreactors for 2-chlorophenol-contained wastewater treatment, Chemosphere. 140 (2015) 79–84. https://doi.org/10.1016/j.chemosphere.2014.04.101.

[22]   V. Diez, A. Iglesias, J.M. Cámara, M.O. Ruiz, C. Ramos, A novel anaerobic filter membrane bioreactor: Prototype start-up and filtration assays, Water Sci. Technol. 78 (2018) 1833–1842. https://doi.org/10.2166/wst.2018.309.

[23]   N. Li, L. He, Y.Z. Lu, R.J. Zeng, G.P. Sheng, Robust performance of a novel anaerobic biofilm membrane bioreactor with mesh filter and carbon fiber (ABMBR) for low to high strength wastewater treatment, Chem. Eng. J. 313 (2017) 56–64. https://doi.org/10.1016/j.cej.2016.12.073.

[24]   K. V. Rajeshwari, M. Balakrishnan, A. Kansal, K. Lata, V.V.N. Kishore, State-of-the-art of anaerobic digestion technology for industrial wastewater treatment,

Renew. Sustain. Energy Rev. 4 (2000) 135–156. https://doi.org/10.1016/S1364-0321(99)00014-3.

[25] G. Skouteris, D. Hermosilla, P. López, C. Negro, Á. Blanco, Anaerobic membrane bioreactors for wastewater treatment: A review, Chem. Eng. J. 198–199 (2012) 138–148. https://doi.org/10.1016/j.cej.2012.05.070.

[26] A. Saddoud, S. Sayadi, Application of acidogenic fixed-bed reactor prior to anaerobic membrane bioreactor for sustainable slaughterhouse wastewater treatment, J. Hazard. Mater. 149 (2007) 700–706. https://doi.org/10.1016/j.jhazmat.2007.04.031.

[27] APHA, Standard Methods for the Examination of Water and Wastewater, 2001.

[28] C. Holliger, M. Alves, D. Andrade, I. Angelidaki, S. Astals, U. Baier, C. Bougrier, P. Buffière, M. Carballa, V. De Wilde, F. Ebertseder, B. Fernández, E. Ficara, I. Fotidis, J.C. Frigon, H.F. De Laclos, D.S.M. Ghasimi, G. Hack, M. Hartel, J. Heerenklage, I.S. Horvath, P. Jenicek, K. Koch, J. Krautwald, J. Lizasoain, J. Liu, L. Mosberger, M. Nistor, H. Oechsner, J.V. Oliveira, M. Paterson, A. Pauss, S. Pommier, I. Porqueddu, F. Raposo, T. Ribeiro, F.R. Pfund, S. Strömberg, M. Torrijos, M. Van Eekert, J. Van Lier, H. Wedwitschka, I. Wierinck, Towards a standardization of biomethane potential tests, Water Sci. Technol. 74 (2016) 2515–2522. https://doi.org/10.2166/wst.2016.336.

[29] M. Raffin, E. Germain, S. Judd, Optimising operation of an integrated membrane system (IMS) - A Box-Behnken approach, Desalination. 273 (2011) 136–141. https://doi.org/10.1016/j.desal.2010.10.030.

[30] P.J. Huber, Robust Statistics, Wiley & Sons, New York, 1981.

[31] H. Liu, C. Yang, W. Pu, J. Zhang, Formation mechanism and structure of dynamic

membrane in the dynamic membrane bioreactor, Chem. Eng. J. 148 (2009) 290–295. https://doi.org/10.1016/j.cej.2008.08.043.

[32]   P. Le Clech, B. Jefferson, I.S. Chang, S.J. Judd, Critical flux determination by the flux-step method in a submerged membrane bioreactor, J. Memb. Sci. 227 (2003) 81–93. https://doi.org/10.1016/j.memsci.2003.07.021.

[33]   R.K. Dereli, A. Grelot, B. Heffernan, F.P. van der Zee, J.B. van Lier, Implications of changes in solids retention time on long term evolution of sludge filterability in anaerobic membrane bioreactors treating high strength industrial wastewater., Water Res. 59C (2014) 11–22. https://doi.org/10.1016/j.watres.2014.03.073.

[34]   H. Chua, W.F. Hu, P.H.F. Yu, M.W.L. Cheung, Responses of an anaerobic fixed-film reactor to hydraulic shock loadings, Bioresour. Technol. 61 (1997) 79–83. https://doi.org/10.1016/S0960-8524(97)84702-5.

[35]   H. Cheng, Y. Li, L. Li, R. Chen, Y.Y. Li, Long-term operation performance and fouling behavior of a high-solid anaerobic membrane bioreactor in treating food waste, Chem. Eng. J. 394 (2020). https://doi.org/10.1016/j.cej.2020.124918.

[36]   M.M. Alves, J.A. Mota Vieira, M. Alvares Pereira, A. Pereira, M. Mota, Effect of Lipids and Oleic Acid on Biomass Development in Anaerobic Fixed-Bed Reactors. Part I : Biofilm Growth and Activity, Water Res. 35 (2001) 255–263.

[37]   J. Ho, S. Sung, Methanogenic activities in anaerobic membrane bioreactors (AnMBR) treating synthetic municipal wastewater, Bioresour. Technol. 101 (2010) 2191–2196. https://doi.org/10.1016/j.biortech.2009.11.042.

[38]   R. Martínez, M.O. Ruiz, C. Ramos, J.M. Cámara, V. Diez, Comparison of external and submerged membranes used in anaerobic membrane bioreactors: Fouling related issues and biological activity, Biochem. Eng. J. 159 (2020) 107558.

https://doi.org/10.1016/j.bej.2020.107558.

[39] M. Harb, Y. Xiong, J. Guest, G. Amy, P.Y. Hong, Differences in microbial communities and performance between suspended and attached growth anaerobic membrane bioreactors treating synthetic municipal wastewater, Environ. Sci. Water Res. Technol. 1 (2015) 800–813. https://doi.org/10.1039/c5ew00162e.

[40] V. Diez, C. Ramos, J.L. Cabezas, Treating wastewater with high oil and grease content using an Anaerobic Membrane Bioreactor (AnMBR). Filtration and cleaning assays, Water Sci. Technol. 65 (2012) 1847–1853. https://doi.org/10.2166/wst.2012.852.

[41] V. Diez, D. Ezquerra, J.L. Cabezas, a. García, C. Ramos, A modified method for evaluation of critical flux, fouling rate and in situ determination of resistance and compressibility in MBR under different fouling conditions, J. Memb. Sci. 453 (2014) 1–11. https://doi.org/10.1016/j.memsci.2013.10.055.

[42] H. Lin, W. Peng, M. Zhang, J. Chen, H. Hong, Y. Zhang, A review on anaerobic membrane bioreactors: Applications, membrane fouling and future perspectives, Desalination. 314 (2013) 169–188. https://doi.org/10.1016/j.desal.2013.01.019.

[43] H. Ozgun, R.K. Dereli, M.E. Ersahin, C. Kinaci, H. Spanjers, J.B. Van Lier, A review of anaerobic membrane bioreactors for municipal wastewater treatment: Integration options, limitations and expectations, Sep. Purif. Technol. 118 (2013) 89–104. https://doi.org/10.1016/j.seppur.2013.06.036.

[44] P.D. Jensen, S.D. Yap, A. Boyle-Gotla, J. Janoschka, C. Carney, M. Pidou, D.J. Batstone, Anaerobic membrane bioreactors enable high rate treatment of slaughterhouse wastewater, Biochem. Eng. J. 97 (2015) 132–141.

https://doi.org/10.1016/j.bej.2015.02.009.

[45]   W. Fuchs, H. Binder, G. Mavrias, R. Braun, Anaerobic treatment of wastewater with high organic content using a stirred tank reactor coupled with a membrane filtration unit, Water Res. 37 (2003) 902–908. https://doi.org/10.1016/S0043-1354(02)00246-4.

[46]   M. Raffin, E. Germain, S.J. Judd, Influence of backwashing, flux and temperature on microfiltration for wastewater reuse, Sep. Purif. Technol. 96 (2012) 147–153. https://doi.org/10.1016/j.seppur.2012.05.030.

[47]   T. Zsirai, P. Buzatu, P. Aerts, S. Judd, Efficacy of relaxation, backflushing, chemical cleaning and clogging removal for an immersed hollow fibre membrane bioreactor, Water Res. 46 (2012) 4499–4507. https://doi.org/10.1016/j.watres.2012.05.004.

[48]   P. Bacchin, P. Aimar, R.W. Field, Critical and sustainable fluxes: Theory, experiments and applications, J. Memb. Sci. 281 (2006) 42–69. https://doi.org/10.1016/j.memsci.2006.04.014.